This will require that the materials grow by a layer-by-layer two-dimensional mechanism to produce structures with coherent interfaces. We are presently exploring the growth mechanism to determine whether the growth is two-dimensional, or if hemispherical nuclei form which follow the orientation of the prelayer. We also plan to use electrocrystallized $Ag(Ag_3O_4)_2NO_3$ single crystals as substrates for electrodeposited superlattices.

Acknowledgment. This work was supported in part by the Division of Materials Research of the National Science Foundation under Grant No. DMR-9020026 and by the Materials Division of the Office of Naval Research under Grant No. N00014-91-J-1499. We also thank Unocal Corp. for donation of electrochemical instrumentation used in this research.

Registry No. $Ag(Ag_3O_4)_2NO_3$, 12258-22-9; $Pb_{0.8}Tl_{0.2}O_{1.9}$, 144224-58-8; $Pb_{0.4}Tl_{0.6}O_{1.7}$, 144224-59-9; Tl_2O_3, 1314-32-5; 430 stainless steel, 11109-52-7.

Clusters of Immiscible Metals. 2. Magnetic Properties of Iron–Lithium Bimetallic Particles

G. N. Glavee,[1] Kathie Easom,[1] K. J. Klabunde,*[,1] C. M. Sorensen,[2] and G. C. Hadjipanayis[3]

Departments of Chemistry and Physics, Kansas State University, Manhattan, Kansas 66506, and Department of Physics and Astronomy, University of Delaware, Newark, Delaware 19716

Received July 7, 1992. Revised Manuscript Received September 9, 1992

Using low-temperature atom clustering processes, metastable Fe–Li nanoscale particles have been prepared. Upon heat treatment further phase segregation occurred, yielding a core-shell structure of α-Fe clusters surrounded by Li metal. Upon oxidation a coating of Li_2O was formed, but α-Fe particles remained and were protected. Upon CO_2 exposure a Li_2CO_3 protective coating was formed. Saturation magnetization σ values ranged from 100 to 200 emu/g and varied slightly with α-Fe crystallite size. However, coercivities were affected more strongly (and showed a maximum at about 7 nm) and ranged from 20 to 1000 Oe. Mössbauer spectra yielded hyperfine fields and isomer shifts for the various samples. Overall, the protective coatings of Li, Li_2O, and Li_2CO_3 had very little effect on α-Fe particle magnetism, and this is in contrast to the effects of coatings of magnetic materials such as Fe_3O_4. On the other hand, crystallite size effects were significant.

Introduction

The controlled generation of nanoscale α-Fe particles encapsulated and protected by a Li_2CO_3/Li_2O coating was discussed in the first of this series on clusters of immisible metals.[4] The synthetic method involves clustering of Fe and Li atoms in low-temperature matrices yielding metastable Fe_xLi_y clusters (solvated metal atom dispersion, SMAD). The advantages of this approach and the utility of materials generated from it have been described elsewhere.[5-8] The unique properties associated with nanoscale particles have been the subject of a number of recent reviews and publications.[9-11] In addition, the properties of magnetic materials, in particular nanoscale iron particles, have been studied extensively in an effort to develop new materials with higher coercivity and saturation magnetization as well as improve recording density.[12,13]

This work examines the soft magnetic properties of nanoscale α-Fe particles encapsulated by Li metal and, after oxidation, of α-Fe particles encapsulated in Li_2CO_3/Li_2O. For comparison, samples of Fe (without Li) were also studied.

Experimental Section

The preparation and thermal and oxidative processing of Fe–Li and Fe (without Li) samples have been described previously.[4] Crystallite sizes were obtained from X-ray powder diffraction data (Scintag 2000 diffractometer with Cu Kα nickel filtered radiation) and particle sizes from transmission electron microscopy and BET surface area (Micrometics, Flowsorb II 2300 utilizing nitrogen adsorption).[4] Ambient- and low-temperature (77 K) Mössbauer spectra were obtained on a Ranger Scientific Inc. MS-1200 using a cryostat designed by Cryo Industries of America, Inc.

Magnetic properties of the fresh and heat processed samples were obtained using a SQUID magnetometer on weighed samples immobilized and protected by encapsulation in paraffin in a quartz cell at temperatures between 10 and 300 K and in fields up to 55 000 Oe. Elemental analyses were obtained from Galbraith Laboratory, Inc. and the analytical laboratory at Kansas State University.

Results and Discussion

(1) Fe–Li (Fresh) Samples. Mössbauer Spectra and Structural Considerations. The fresh Fe–Li sample has been previously described as a "plum-pudding" structure

(1) Kansas State University, Department of Chemistry.
(2) Kansas State University, Department of Physics.
(3) University of Delaware.
(4) Glavee, G. N.; Kernizan, C. F.; Klabunde, K. J.; Sorensen, C. M.; Hadjipanayis, G. C. *Chem. Mater.* **1991**, *3*, 967.
(5) Klabunde, K. J.; Tanaka, Y. *J. Mol. Catal.* **1983**, *21*, 57.
(6) Klabunde, K. J.; Jeong, G. H.; Olsen, A. W. *Selective Hydrocarbon Activation: Principles and Progress*; Davies, J. A., Watson, P. L., Greenberg, A., Liebman, J. F., Eds.; VCH Publishers: New York, 1990; Chapter 13, pp 433.
(7) Kernizan, C. F.; Klabunde, K. J.; Sorensen, C. M.; Hadjipanayis, G. C. *Chem. Mater.* **1990**, *2*, 70.
(8) Klabunde, K. J.; Davis, S. C.; Hattori, H.; Tanaka, Y. *J. Catal.* **1978**, *54*, 254.
(9) Andres, R. P.; Averback, R. S.; Brown, W. L.; Brus, L. E.; Goddard III, W. A.; Kaldor, A.; Louie, S. G.; Moskovits, M.; Riley, S. T.; Siegal, R. W.; Spaepen, F.; Wang, Y. *J. Mater. Res.* **1989**, *4*, 704.
(10) Matijevic, E. Fine Particles: Science and Technology. *MRS Bull.* **1989**, *14*, 19. Matijevic, E. Fine Particles Part II: Formation Mechanisms and Applications. *MRS Bull.* **1990**, 15, 20.
(11) Ozaki, M. *MRS Bull.* **1989**, *14*, 35.
(12) (a) Tasaki, A.; Tomiyana, S.; Iida, S. *J. J. Appl. Phys.* **1965**, *4*, 707. (b) Hayashi, C. *J. Vac. Sci. Technol. A* **1987**, *5*, 1375.
(13) (a) Nakatani, I.; Furubayashi, T.; Takahashi, T.; Hanoaka, H. *J. Magn. Magn. Mater.* **1987**, *65*, 261. (b) Tang, Z. X.; Nafis, S.; Sorensen, C. M.; Hadjipanayis, G. A.; Klabunde, K. J. *J. Magn. Magn. Mater.* **1989**, *80*, 285. (c) Nafis, S.; Hadjipanayis, G. C.; Sorensen, C. M.; Klabunde, K. J. *IEEE Trans. Magn.* **1989**, *25*, 3641.

0897-4756/92/2804-1360$03.00/0

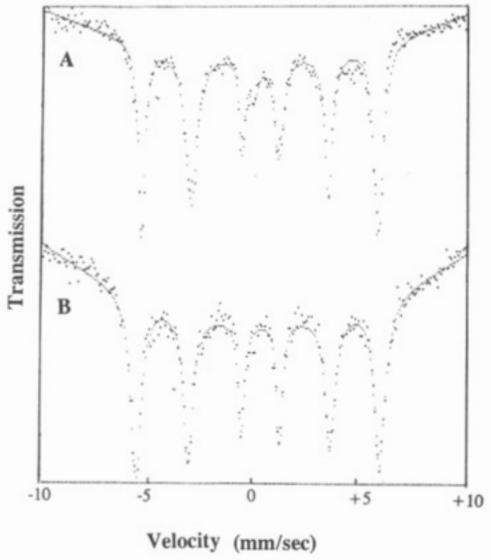

Figure 1. Mössbauer spectra at 77 K of fresh (A) Fe–Li and (B) Fe (without Li) samples.

which consists of very small α-Fe crystallites imbedded in a large nanocrystalline Li matrix with some of the matrix material (pentane) trapped inside.[4] Despite the small crystallite size (about 3 nm) for these imbedded α-Fe crystallites, we observed a distinct sextet in the ambient-temperature Mossbauer spectrum which suggests that the regions of α-Fe are large enough to exhibit long-range magnetic interactions.[4] However, there also exists a superparamagnetic component as evidenced by a broadening in the center of the spectrum near zero velocity.[14] The spectrum simplifies at 77 K to yield mainly a sextet corresponding to α-Fe (Figure 1A).

Thus, the low-temperature Mossbauer studies confirm our earlier conclusion that these Fe–Li (fresh) samples consist of partially phase-separated aggregates with α-Fe crystallites imbedded in a Li metal matrix (Scheme I). A small superparamagnetic fraction is present most likely due to the presence of extremely small α-Fe clusters. However, considering the time scale of the Mossbauer measurement ($\sim 10^{-7}$ s), it would be expected that the crystallites would have to be greater than 7.0 nm at 300 K or 4.5 nm at 10 K to exhibit ferromagnetism resulting in six lines in the Mossbauer spectrum.[15] Therefore, it

Scheme I. Fe–Li Particles "Plum Pudding" Structure

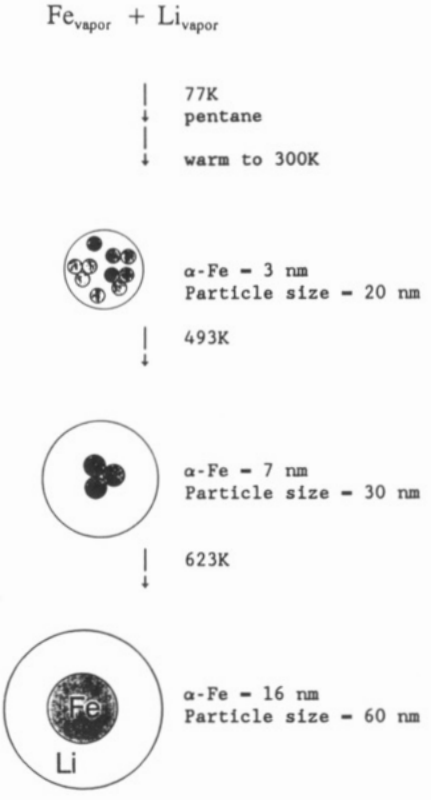

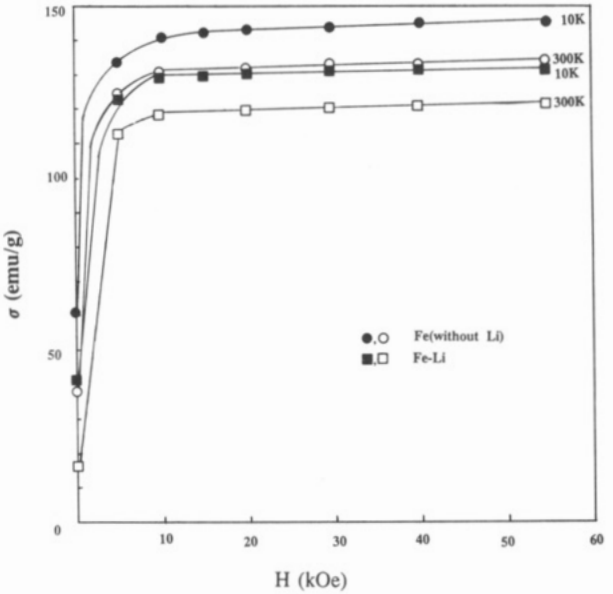

Figure 2. Saturation magnetization (σ) as a function of applied field for fresh Fe–Li and Fe (without Li) samples.

becomes clear that the small crystallites imbedded in the Li matrix must be magnetically interacting, which would require their very close proximity. Thus, the best picture of this revised plum pudding model is shown in Scheme I, where three or four crystallites are aggregated together. In this structure, magnetic interactions should be possible between the crystallites.

Magnetic Properties. The magnetization curves for fresh Fe–Li and Fe (without Li) samples are shown in Figure 2. Saturation magnetizations of 132 and 122 emu/g were obtained for Fe–Li particles at 10 and 300 K respectively. For Fe (without Li) particles the values were 146 and 135. However, since these are on a per gram basis, the percent Fe of the total weight needs to be taken into

(14) (a) Papaefthymiou, V.; Kostikas, A.; Simopoulos, A.; Niarchos, D.; Gangopadhyay, S.; Hadjipanayis, G. C.; Klabunde, K. J.; Sorensen, C. M. *J. Appl. Phys.* **1990**, *67*, 4487. (b) Hayashi, M.; Tamura, I.; Fukano, Y.; Kanemaki, S. *Surf. Sci.* **1981**, *106*, 453.

(15) The characteristic time τ for reversal of the magnetization in an assembly of uniaxial particles of volume V with anisotropy constant k is given by Cullity (Cullity, B. D. *Introduction to Magnetic Materials*; Addison-Wesley Publishing Co.: Reading, MA, 1972; 410–422) as

$$\tau^{-1} = f_0 e^{-KV/k_B T} \quad (1)$$

Where $k_B T$ is the thermal energy and $f_0 = 10^9$ s^{-1}. Superparamagnetism for a given type of measurement, e.g., Mössbauer or magnetrometry, occurs when this characteristic time is comparable to the time scale of the measurement. For magnetometry, the measurement time scale is ca. 10^2 s, whereas for Mössbauer it is ca. 10^{-7} s. Equation 1 can be solved for V and τ set equal to either of these time scales to obtain the superparamagnetic size, below which the particles are superparamagnetic, for either measurement as a function of temperature. We find

$$d \simeq V^{1/3} \simeq [k_B T k^{-1} \ln \tau f_0]^{1/3} \quad (2)$$

The anisotropy constant for iron varies somewhat with temperature, K(77 K) = 5.6×10^5 erg/cm^2, k(300 K) = 4.8×10^5 erg/cm^2. Thus we can calculate the superparamagnetic sizes for magnetometry as d(77 K) $\simeq$ 80 Å, d(300 K) $\simeq$ 130 Å and for Mossbauer as d(77 K) $\simeq$ 44 Å, d(300 K) $\simeq$ 74 Å.

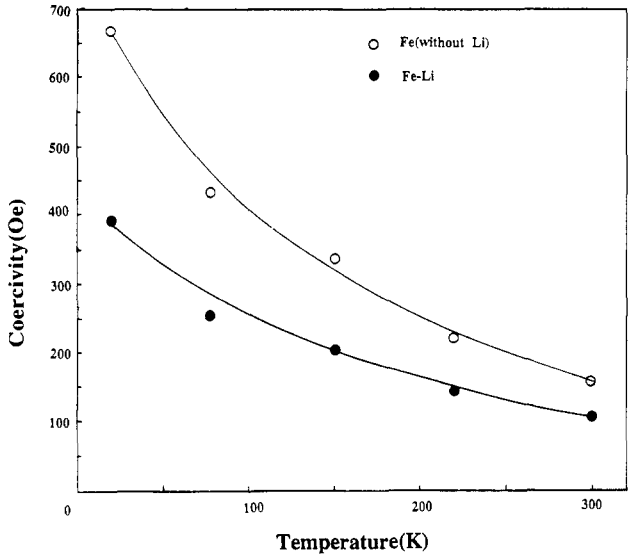

Figure 3. Coercivity as a function of sample (SQUID) temperature for fresh Fe–Li and Fe (without Li) samples.

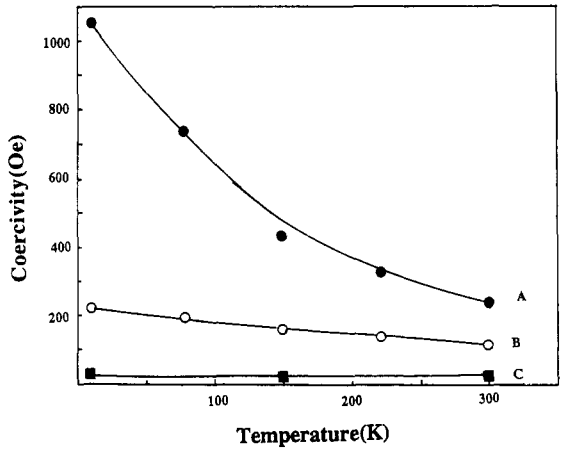

Figure 4. Coercivity as a function of sample (SQUID) temperature for Fe–Li samples heat treated at different temperatures for 60 min, followed by oxidation of lithium. (A) 493 K; (B) 623 K; (C) 898 K.

account; that for Fe–Li is 74% and for Fe (without Li) 90%. The corrected saturation magnetizations per gram (emu/g) Fe become

	σ	
T, K	Fe–Li	Fe (without Li)
10	178	162
300	164	150

The temperature dependence of the coercivity of Fe–Li and Fe (without Li) particles is shown in Figure 3. It is clear that coercivities are slightly lower for the Fe–Li sample.

Since our work on related systems has led to the synthesis of several coated α-Fe nanoscale particles, it is interesting to compare these different materials. Therefore Table I compares coercivities obtained for similar α-Fe crystallite sizes from SMAD generated Fe–Li, Fe (without Li) and Fe/FeS samples as well as Fe/Fe_3O_4 generated by deposition of Fe into an inert atmosphere gas (argon). The unusually high coercivities and strong temperature dependence of the Fe/Fe_3O_4 samples is attributed to a combination of small particle size, interaction of the superparamagnetic granular shell with the metallic iron core, and magnetic dipole interactions among the small particles.[16] In contrast, Fe (without Li) samples, in which

Table I. Comparison of Coercivities of Fe (without Li), Fe/Li, Fe/Fe_3O_4, and Fe/FeS Samples

samples	α-Fe crystallite size (nm)	coercivity at 10 K (Oe)	saturation magnetization (emu/g)
Fe (without Li)	~2.0	670 (157)[b]	146 (135)[b]
Fe–Li	~3.0	395 (110)[b]	132 (122)[b]
Fe/Fe_3O_4[c]	2.5	3400 (0)[a]	25
	3.3	2400 (31)[a]	52
Fe/FeS[d]	<5	1000 (200)[b]	78 (75)[b]
	<10	1075 (530)[b]	117 (112)[b]
bulk α-Fe		≤50	220[a,b]

[a] Values in parentheses obtained at 150 K. [b] Values in parentheses obtained at 300 K. [c] Work of S. Gangopadhyay.[16] [d] Unpublished work of Kathie Eason from this laboratory.

Table II. Ambient Temperature Mössbauer Data on Fe–Li Samples Heat Processed at Different Temperatures followed by Oxidation of Lithium

sample[a]	isomer shift[b,e] (mm/s)	QS[c] (mm/s)	hyperfine field[b,c] (kOe)
Fe–Li (fresh)	−0.02 [0.22]	1.6	322
Fe–Li (493 K)	−0.04 [0.24]	1.6	329
Fe–Li (623 K)	0.01 (0.12)		329 (206)
Fe–Li (898 K)	−0.02		330

[a] Sample heat treated under argon at the temperature indicated for 60 min. [b] Numbers in parentheses refer to the carbide component. [c] Error limits: isomer shift ±0.02 mm/s; QS ± 0.04 mm/s; hyperfine field ±8 kOe. [d] Relative to bulk α-Fe. [e] Numbers in brackets refer to central doublet.

Table III. Mössbauer Data at 77 K on Fe–Li Samples Heat Processed at Different Temperatures followed by Oxidation of Lithium

sample	isomer shift[b,c] (mm/s)	hyperfine field[b,c] (kOe)
Fe–Li (fresh)	0.02	335
Fe–Li (493 K)	0.09	334
Fe–Li (623 K)	0.05 (0.22)	333 (241)

[a] Sample heat treated under argon at the noted temperature for 60 min. [b] Numbers in parentheses refer to the carbide component. [c] See Table II for error limits.

successful efforts were made to minimize oxidation in both the SQUID and Mossbauer studies do not show the unusually high coercivities nor the drastic temperature dependence. An even lower coercivity was observed for the Fe–Li sample suggesting that the interaction of the Fe and Li is weak and certainly does not enhance coercivity.

Another way to evaluate if there is a significant iron–lithium magnetic interaction is by measuring hyperfine fields (kOe) in the Mössbauer, and these are shown below (also see Tables II and III):

	293 K	77 K
Fe–Li (fresh)	322	335
Fe (without Li)	325	337
bulk α-Fe	330	333

Since the errors in the these numbers are ±5 kOe, it would appear that the presence of Li essentially has no effect on the hyperfine fields.

(2) Heat Processed Samples Followed by Controlled Oxidation. *Mössbauer Spectra and Structural Considerations.* Thermal processing results in a core-shell structure with the core composed of α-Fe, but some Fe_3C

(16) (a) Gangopadhayay, S.; Hadjipanayis, G. C.; Dale, B.; Sorensen, C. M.; Klabunde, K. J.; Papaefthymiou, V.; Kostikas, A. *Phys. Rev. B* **1992**, *45*, 9778. (b) Papaefthymiou, V.; Kostikas, A.; Simopoulos, A.; Niarchos, D.; Gangopadhyay, S.; Hadjipanayis, G. C.; Klabunde, K. J.; Sorensen, C. M. *Proc. 3M Conf. Boston 1989.* (c) Gong, W.; Li, H.; Zhao, Z.; Chen, J. *J. Appl. Phys.* **1991**, *69*, 5119.

Table IV. Saturation Magnetization (σ), Coercivity, and α-Fe Crystallite Sizes of Fe–Li Samples (Fresh and Heat Processed at Various Temperatures followed by Lithium Oxidation)

sample[a]	σ (emu/g)		σ (emu/g of iron)		coercivity		
	10 K	300 K	10 K	300 K	10 K	300 K	crystallite size (nm)
Fe–Li (fresh)	132	122	178	164	395	110	3.3
Fe–Li (493 K)	37	33	106	103	1050	250	7.3
Fe–Li (623 K)	80	76	216	205	220	115	16
Fe–Li (898 K)	134	128	191	183	28	20	33
Fe (without Li, fresh)	142	135	158	150	670	157	2.0
Fe (without Li, 573 K)	151	135	168	150	810	370	14
Fe (without Li, 743 K)	143	125	159	139	505	220	28

[a] Sample heat treated under argon at the indicated temperature for 60 min.

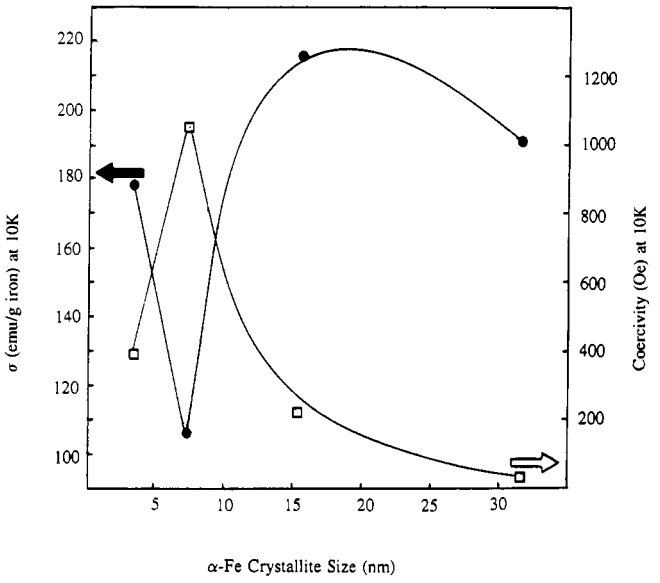

Figure 5. Coercivity and saturation magnetization (σ) plotted against α-Fe crystallite size (measurements at 10 K). (●) σ; (□) coercivity (H_c).

also was detected at specific (743 K) heat treatment temperatures.[4,17] Crystallite sizes for α-Fe increased in a controllable way with temperature increase, showing that particle sintering was taking place (Scheme I). Upon oxygen exposure, the Li metal was oxidized, and upon extended exposure to the atmosphere, the Li_2O was converted to Li_2CO_3 due to CO_2 in the air.

For comparison a sample of Fe (without Li) was prepared by the same method (iron atom clustering in cold pentane) and heat processed. Figure 1B shows that the Fe (without Li, fresh) consists of α-Fe particles. However, oxygen exposure for this sample caused formation of Fe_2O_3 since no protective coating was present.

Magnetic Properties of Thermally Processed Fe–Li Samples. Saturation magnetization (σ) of heat-processed Fe–Li samples passed through a minimum (493 K heat treatment, 7.3-nm α-Fe crystallites, see Table IV). Upon further heating σ increased again (Figure 5). The opposite behavior was encountered for coercivity (H_c), and it went through a maximum at the 7.3-nm crystallite size. And it is important to note that the same trends were observed at 10 and 300 K, and this is in contrast to results found for α-Fe particles coated with small grained, superparamagnetic Fe_3O_4 where Hc varied in opposite directions at 10 vs 300 K.[16] These results with the Fe–Li system show convincingly that the protective Li_2O/Li_2CO_3 coating has no significant effect on the magnetic properties of the inner α-Fe core.

One confusing issue remains, however. It would be expected that maximum coercivity would be observed for α-Fe crystallites of a size approaching the single domain size of α-Fe, which is 20–22 nm.[16] As mentioned before and illustrated in Scheme I, we believe that the α-Fe crystallites may be imbedded near each other allowing magnetic interactions. In this way, perhaps about three 7.3-nm crystallites formed by heat treatment at 493 K are, on average, close enough to magnetically communicate with each other. It seems that this would be possible within an overall particle diameter of about 30–35 nm.[4]

Concluding Remarks

Metastable Fe–Li particles can be prepared at low temperatures. At 77 K in pentane partial phase segregation yields α-Fe crystallites of varying sizes with an upper limit of 3 nm. Thermal treatments cause further phase segregation yielding a more pronounced core-shell structure (iron crystallites surrounded by lithium).

Higher temperature heat treatments cause particle sintering so that larger analogous core-shell structures are obtained. Crystallite size of α-Fe can be controlled by temperature and time. However, at intermediate temperatures Fe_3C is observed as well.

Oxidation of the Fe–Li particles yields α-Fe crystallites coated and protected first by a Li_2O shell that eventually forms a Li_2CO_3 shell. The α-Fe crystallites are stable for months in the air at ambient temperatures.

In general, the coercivity of the heat processed/oxidized Fe–Li samples varies inversely with saturation magnetization. The Li, Li_2O, or Li_2CO_3 coatings have little or no influence on the magnetic properties of the α-Fe metallic core of the particles. This is particularly evident from the Mossbauer data (Table II).

The best representation of particle structure is a "plum-pudding" model with some α-Fe crystallites close enough to magnetically interact.

Acknowledgment. The support of the National Science Foundation through its Materials Chemistry initiative is acknowledged with gratitude.

Registry No. Fe, 7439-89-6; Li, 7439-93-2; Li_2O, 12057-24-8; Li_2CO_3, 554-13-2.

(17) We have shown that Fe_3C only forms when the temperature of heat treatment approaches the 743 K range, and then decomposes upon heating much above 800 K. Therefore, Fe_3C was only detected in significant amounts at 743 K. Due to the magnetic effects of the Fe_3C, we have not included the data points for this temperature in Table IV or Figure 5.